Structural Engineering and Mechanics, Vol.1, No.1 (1993) 119-135
DOI: http://dx.doi.org/10.12989/sem.1993.1.1.119

Generalized optimal active control algorithm with weighting matrix configuration, stability and time-delay

Franklin Y. Cheng †

Intelligent Systems Center

Peter Tian ‡

Civil Engineering Department, University of Missouri-Rolla, MO 65401, USA

Abstract. The paper presents a generalized optimal active control algorithm for earthquake-resistant structures. The study includes the weighting matrix configuration, stability, and time-delays for achieving control effectiveness and optimum solution. The sensitivity of various time-delays in the optimal solution is investigated for which the stability regions are determined. A simplified method for reducing the influence of time-delay on dynamic response is proposed.

Numerical examples illustrate that the proposed optimal control algorithm is advantageous over others currently in vogue. Its feedback control law is independent of the time increment, and its weighting matrix can be flexibly selected and adjusted at any time during the operation of the control system. The examples also show that the weighting matrix based on pole placement approach is superior to other weighting matrix configurations for its self-adjustable control effectiveness. Using the time-delay correction method can significantly reduce the influence of time-delays on both structural response and required control force.

Key words: active control; dynamic structures; earthquakes; optimal control algorithm; pole placement technique; stability analysis; time-delay.

1. Introduction

Several algorithms for optimal active control of seismic structures have been developed. Among them, the algebraic Riccati algorithm was studied by Abdel-Rohman (1980), Yang (1985) and Cheng (1988), and the instantaneous optimum active control (IOAC) algorithm was early proposed by Yang (1987), and studied by Soong (1987) and Cheng (1986, 1987, 1988). Recent studies by Cheng (1991) reveal that in the IOAC closed-loop control algorithm the feedback gain matrix is very sensitive to incremental time intervals used in response analysis. For a given structure subjected to certain earthquake loading, using different time intervals may yield various control forces and structural responses. The results are apparently not unique. A technique called generalized optimal active control (GOAC) algorithm was conse-

† Senior Investigator, Curators' Professor of Civil Engineering
‡ Ph. D. Candidate

quently devseloped for linear and nonlinear seismic structures (Cheng 1991, 1992) and is further studied in this paper.

In optimal active control algorithms, the optimal control forces are usually achieved through trial and error of weighting matrices. For a multistory building structure equipped with control at different floors, the dimensions of weighting matrices are numerous. Therefore it is cumbersome to try all possible combinations of elements in these matrices to obtain the optimum solution. For simplicity, diagonal weighting matrices are usually assumed. However, it will be shown in this paper that the diagonal assumption may not lead to the optimum solution.

Studies also indicate that the dominant frequency of dynamic loading influences the control effectiveness. For a given control law, the control effectiveness could change when different external excitations are applied. Since both algebraic Riccati and IOAC algorithms are derived without considering the frequency of external excitations, this factor has been omitted from the control laws of these algorithms.

In this paper, the function of weighting matrix in the control law of a closed-loop control system is studied for its effectiveness based on the pole placement approach (Ogata 1990). With this approach, the desired eigenvalues of the closed-loop system need to be selected. Since the eigenvalues can be expressed in terms of frequencies and damping ratios, the desired parameters can be properly chosen in order to avoid resonance and large amplitude of structural response.

The study also includes stability regions influenced by time delays. Two types of time delays are considered: one is called on-line computation time delay, represented by t_x and $t_{\dot{x}}$, which is caused by sensoring the structural response and computing the required control force; the other is called control force build-up time delay, signified by α or t_b, which is the time required for a mechanical system to build up a control force. The influence of the time-delays on dynamic response is corrected on the basis that the time-delays can be considered as phase angle lags for displacement and velocity, and the effects of time-delays are mainly applied to dynamic response of the floors adjacent to the active control location.

2. Formulations of generalized optimal active control algorithm

2.1. Motion equation for active tendon control system

The motion equation for a plane N-story seismic structure equipped with active tendons at some floors, as shown in Fig. 1, can be expressed as

$$[M]\{\ddot{x}(t)\}+[C]\{\dot{x}(t)\}+[K]\{x(t)\} = [\gamma]\{u(t)\}+\{\delta\}\ddot{X}_g(t) \tag{1}$$

where, $[M]$, $[C]$ and $[K]$ of $N\times N$ are mass, damping, and stiffness matrices of the building structure, respectively; $\{x(t)\}$ of $N\times 1$ and $\{u(t)\}$ of $r\times 1$ are vectors of the relative displacement of the structure and the control forces of the active tendons, respectively, where r is the number of active tendons; $[\gamma]$ of $N\times r$ is location matrix for the control forces of the active tendons; and $\{\delta\}$ of $N\times 1$ is the coefficient vector for the earthquake ground acceleration, $\ddot{X}_g(t)$.

By defining the state vector

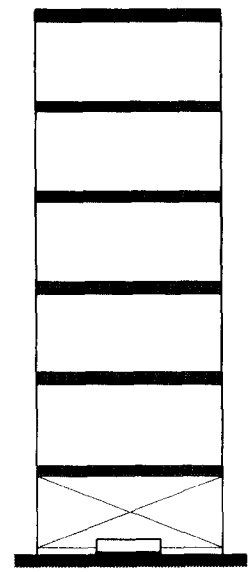

Fig. 1 Active Tendon Control System

$$\{z(t)\} = \begin{Bmatrix} \{x(t)\} \\ \{\dot{x}(t)\} \end{Bmatrix} \tag{2}$$

Eq. (1) can be changed to the following state form

$$\{\dot{z}(t)\} = [A]\{z(t)\} + [B]\{u(t)\} + \{C'\}\ddot{X}_g(t) \tag{3}$$

where

$$\left.\begin{aligned} \{z(t)\} &= \begin{Bmatrix} \dot{x}(t) \\ \ddot{x}(t) \end{Bmatrix}_{2N\times 1} \\ [A] &= \begin{bmatrix} [0] & [I] \\ -[M]^{-1}[K] & -[M]^{-1}[C] \end{bmatrix}_{2N\times 2N} \\ [B] &= \begin{bmatrix} [0] \\ [M]^{-1}[\gamma] \end{bmatrix}_{2N\times r} \\ [C'] &= \begin{bmatrix} \{0\} \\ [M]^{-1}\{\delta\} \end{bmatrix}_{2N\times 1} \end{aligned}\right\} \tag{4}$$

The corresponding initial conditions in state form are

$$\{z(0)\} = \{0\},\ \{u(0)\} = \{0\},\ \text{and}\ \ddot{X}_g(0) = 0 \tag{5}$$

2.2. Generalized performance index

In order to obtain an optimal solution for state vector $\{z(t)\}$ and control force vector $\{u(t)\}$, a performance index needs to be defined and minimized. The standard quadratic per-

formance index is expressed as

$$J = \frac{1}{2}\int_{t_0}^{t_f} (\{z(t)\}^T [Q]\{z(t)\} + \{u(t)\}^T [R]\{u(t)\})dt \tag{6}$$

in which $[Q]$ of $2N \times 2N$ is a positive semidefinite matrix; $[R]$ of $r \times r$ is a positive definite matrix; t_0 is the initial and t_f the final time-instant under consideration. The duration between t_0 and t_f should be defined as longer than that of the earthquake.

By dividing the duration $[t_0, t_f]$ into n segments, Eq. (6) can be written as

$$J = \sum_{i=1}^{n} \frac{1}{2}\int_{t_{i-1}}^{t_i} (\{z(t)\}^T [Q]\{z(t)\} + \{u(t)\}^T [R]\{u(t)\})dt \tag{7}$$

It is noted that in Eq. (6) both of the two boundary values of the integrand are specified, i.e., $\{z(t_0)\} = \{z(t_f)\} = \{0\}$ and $\{u(t_0)\} = \{u(t_f)\} = \{0\}$, while in Eq. (7) for each integration from t_{i-1} to t_i $(i = 1, 2, \cdots, n)$, at least one of the two boundary values is unspecified. Therefore the performance index J, defined by Eq. (6), corresponds to a fixed end-point boundary value problem, while the other J, defined by Eq. (7), is related to a free end-point boundary value problem (Citron 1969).

Suppose that the performance index, J, is integrated step by step, and at each step "i", the initial value of the state vector, $\{z(t_{i-1})\}$, is specified from the previous step, but the final value, $\{z(t_i)\}$, is unknown. Hence, $\{z(t_i)\}$ should also be minimized, i.e., a function of $\{z(t_i)\}$ should be included in the expression of the performance index. For this reason, a new performance index defined at the time interval $[t_{i-1}, t_i]$, is selected as follows (Cheng 1991, 1992)

$$\begin{aligned} J_i &= g(\{z(t_i)\}) + \frac{1}{2}\int_{t_{i-1}}^{t_i} (\{z(t)\}^T[Q]\{z(t)\} + \{u(t)\}^T[R]\{u(t)\})dt \\ &= g(\{z(t_i)\}) + \frac{1}{2}\int_{t_{i-1}}^{t_i} \bar{f}(t)dt \end{aligned} \tag{8}$$

where $g(z\{t_i\})$ could be chosen in the form of

$$g(z\{t_i\}) = \frac{1}{2}\{z(t_i)\}^T [S]\{z(t_i)\} \tag{9}$$

in which $[S]$ of $2N \times 2N$ is a positive semi-definite matrix.

It is noted that J_i defined by Eq. (8) will be identical to the standard form of J given in Eq. (6) if t_{i-1} and t_i are chosen to be t_0 and t_f, respectively. Therefore J_i is called generalized performance index.

2.3. Transversality conditions

Since the problem involved is a free end-point boundary value problem, in order to minimize the generalized performance index, J_i, not only Euler equation but also transversality conditions should meet at end-point t_i. Suppose that the end conditions relating the variables

at the end-points are given by

$$\left.\begin{aligned} t_{i-1} &= t_0 + \sum_{k=1}^{i-1} \Delta t_k \\ \{z(t_{i-1})\} &= \{z_{i-1}\} \\ t_i &= t_0 + \sum_{k=1}^{i} \Delta t_k \end{aligned}\right\} \tag{10}$$

where Δt_k is the time increment for the kth segment of the time duration $[t_0, t_f]$, since different time segments can have time increments of different values. Eq. (10) can also be written in the following form

$$\{\Omega\} = \left\{ \begin{matrix} \Omega_1 \\ \{\Omega_2\} \\ \Omega_3 \end{matrix} \right\} = \left\{ \begin{aligned} &(t_{i-1} - t_0) - \sum_{k=1}^{i-1} \Delta t_k \\ &\{z(t_{i-1})\} = \{z_{i-1}\} \\ &(t_i - t_0) - \sum_{k=1}^{i} \Delta t_k \end{aligned} \right\} \tag{11}$$

By introducing multipliers $\{\mu\}$ and $\{\lambda(t)\}$ and forming the following augmented functions

$$G = g(z\{t_i\}) + \{\mu\}^T \{\Omega\} \tag{12}$$

$$\begin{aligned} F(t) = {} & \{z(t)\}^T [Q]\{z(t)\} + \{u(t)\}^T [R]\{u(t)\} \\ & + \{\lambda(t)\}^T ([A]\{z(t)\} + [B]\{u(t)\} + \{C'\}\ddot{X}_g(t) - \{\dot{z}(t)\}) \end{aligned} \tag{13}$$

the tranversality condition can be expressed as

$$dG - \left(\left\{ \frac{\partial F(t)}{\partial \{\dot{z}(t)\}} \right\}^T \{\dot{z}(t)\} - F(t) \right) dt \Big|_{t_{i-1}}^{t_i} + \left\{ \frac{\partial F(t)}{\partial \{\dot{z}(t)\}} \right\}^T d\{z(t)\} \Big|_{t_{i-1}}^{t_i} = 0 \tag{14}$$

Substitution of Eqs. (12) and (13) into Eq. (14) yields

$$[S]\{z(t_i)\} - \{\lambda(t_i)\} = \{0\} \tag{15}$$

2.4. Determination of feedback gain matrix

By applying Euler equation in Eq. (13), the following expression of control force can be obtained

$$\{u(t)\} = -[R]^{-1} [B]^T \{\lambda(t)\} \tag{16}$$

For a closed-loop control system, the relation between the state vector $\{z(t)\}$ and the control force vector $\{u(t)\}$ can be given by

$$\{u(t)\} = [G]\{z(t)\} \tag{17}$$

where $[G]$ is called feedback gain matrix. Since Eqs. (16) and (17) hold at every end-point $t = t_i$ $(i = 1, 2, \cdots, n)$, substituting the transversality conditions Eq. (15) into Eq. (16) and comparing with Eq. (17) gives the expression of feedback gain matrix

$$[G] = -[R]^{-1} [B]^T [S] \tag{18}$$

which is valid at every end-point t_i.

It is noted that the feedback gain matrix $[G]$ shown in Eq. (18) is neither a function of time t_i nor a function of time increment Δt_i. Therefore, during the computation process, Δt_i can be arbitrarily changed within the range of precision. It is also noted that if $[S]$ is chosen to be the algebraic Riccati matrix $[P]$, i.e., let $[S]=[P]$, the feedback gain matrix will be of the form

$$[G] = -[R]^{-1}[B]^T[P] \tag{19}$$

which is identical to the feedback gain matrix of the Riccati closed-loop control algorithm. Therefore the Riccati closed-loop control algorithm is also included in this generalized algorithm.

2.5. Solution technique

Substitution of Eqs. (17) and (18) into the motion equation, Eq. (3), yields

$$\{\dot{z}(t)\} = [D]\{z(t)\} + \{C'\}\ddot{X}_g(t) \tag{20}$$

where $[D]$ is the plant matrix of the closed-loop system defined by

$$[D] = [A] - [B][R]^{-1}[B]^T[S] \tag{21}$$

Let $\{z(t)\}$ be expressed in terms of the modal transformation matrix, $[T]$, of the closed-loop plant matrix, $[D]$, i.e.,

$$\{z(t)\} = [T]\{\psi(t)\} \tag{22}$$

in which $[T]$ has the following property

$$[T]^{-1}[D][T] = [\phi] \tag{23}$$

where elements of $[\phi]$ are eigenvalues of the plant matrix $[D]$. Substituting Eq. (22) into Eq. (20) and premultiplying by $[T]^{-1}$ yields

$$\{\dot{\psi}(t)\} = [\phi]\{\psi(t)\} + \{\Gamma(t)\} \tag{24}$$

where

$$\{\Gamma(t)\} = [T]^{-1}\{C'\}\ddot{X}_g(t) \tag{25}$$

Corresponding initial conditions are

$$\{\psi(0)\} = \{0\},\ \{u(0)\} = \{0\},\ \text{and}\ \ddot{X}_g(0) = 0 \tag{26}$$

The solution of Eq. (24) is given by

$$\{\psi(t)\} = \int_0^t \exp([\phi](t-\tau))\{\Gamma(\tau)\}d\tau \tag{27}$$

which can be performed by numerical integration. After $\{\psi(t)\}$ is determined, $\{z(t)\}$ and $\{u(t)\}$ can be obtained by using Eqs. (22) and (17), respectively.

3. Determination of the weighting matrix [S]

It is found that in this generalized optimal closed-loop control algorithm, optimum solution is assured through selecting optimum weighting matrices [S] and [R]. Traditionally, optimum weighting matrices are searched only by trial-and-error. Since the dimensions of the weighting matrices are numerous ($2N \times 2N$ for [S] and $r \times r$ for [R]), it is cumbersome to try all possible combinations of the elements in these matrices to obtain the optimum solution. Therefore, some simplified assumptions can be made. For example, assume that [S] and [R] are diagonal matrices and all the diagonal elements in a matrix have the same value. However, this may not yield the optimum solution. Herein a better technique of searching for optimum solutions is suggested.

3.1. Further discussion of feedback gain matrix

Let [S] be expressed in the form of submatrices as

$$[S] = \begin{bmatrix} [S_{11}] & [S_{12}] \\ [S_{21}] & [S_{22}] \end{bmatrix} \tag{28}$$

If there is only one active tendon control installed on the ith floor of a structure, i.e., $[R] = r$, Eq. (18) can be expressed as

$$[G] = [[G_1] \mid [G_2]] = \left[-\frac{1}{r}\{\gamma\}^T [M]^{-1} [S_{21}] - \frac{1}{r}\{\gamma\}^T [M]^{-1} [S_{22}] \right] \tag{29}$$

Assume that the elements in the ith row of [S_{21}] and [S_{22}] are the only non-zero elements in [S_{21}] and [S_{22}] (this assumption will not produce any approximation since [S_{21}] and [S_{22}] are not unique matrices). The elements of the submatrices [G_1] and [G_2] can then be written as

$$(G_1)_j = \frac{1}{m_i}\frac{(S_{21})_{ij}}{r} \quad \text{and} \quad (G_2)_j = \frac{1}{m_i}\frac{(S_{22})_{ij}}{r} \quad (j = 1, 2, \cdots, N) \tag{30}$$

Hence, the expression of the control force $u(t)$ can be obtained as

$$u(t) = \frac{1}{rm_i} \sum_{j=1}^{N} \left((S_{21})_{ij}\, x_j(t) + (S_{22})_{ij}\, \dot{x}_j(t)\right) \tag{31}$$

which reveals the influence of the elements of the weighting matrix [S] on the control force $u(t)$. It is found that the effect of relative displacements $x_j(t)$ on $u(t)$ depends solely on the ith row elements of [S_{21}], and the effect of $\dot{x}_j(t)$ on $u(t)$ depends solely on the ith row elements of [S_{22}], and that [Q], [S_{11}], [S_{12}] and the elements $(S_{21})_{lj}$ and $(S_{22})_{lj}$ $(l \neq i)$ do not influence the value of $u(t)$. Hence, trial-and-error is only necessary among the ratios $(S_{21})_{ij}/r$ and $(S_{22})_{ij}/r$.

3.2. Pole placement technique

Although the optimum solution can be tried by assuming that the ith row elements of [S_{21}] and [S_{22}] are identical, i.e.,

$$(S_{21})_{ij} = (S_{22})_{ij} = S_0 \quad (j = 1, 2, \cdots, N) \tag{32}$$

numerical studies indicate that for some cases the distribution of the ith rows of $[S_{21}]$ and $[S_{22}]$ is crucial, and identical elements may not lead to the optimum solution for achieving an effective control system. In order to obtain a good distribution of the ith row of $[S_{21}]$ and $[S_{22}]$ and improve control effectiveness, the following approach, called pole placement technique (Odaga 1990), can be used. The pole placement approach begins by selecting $2N$ values $\bar{\lambda}_1, \bar{\lambda}_2, \cdots, \bar{\lambda}_{2N}$ as the desired closed-loop poles (i.e., eigenvalues of the closed-loop system). Determination of the desired closed-loop poles is based on structural transient and frequency response requirements, such as displacement, velocity, damping ratio and bandwidth.

It can be proven that the desired closed-loop poles may be arbitrarily chosen if the system is completely state controllable, i.e., the rank of the controllability matrix defined by

$$[U] = [\ \{B\} \ \vdots\ [A]\{B\} \ \vdots\ [A]^2\{B\} \vdots \cdots \vdots\ [A]^{2N-1}\{B\}\ ]_{2N\times 2N} \tag{33}$$

is equal to $2N$, or the inverse of $[U]$ exists (Ogata, 1990). In Eq. (33), $[A]$ and $\{B\}$ are, respectively, the plant matrix of the open-loop system and the control force influence vector defined by Eq. (4).

After choosing the $2N$ desired closed-loop poles, the non-zero ratios, $(S_{21})_{ij}/r$ and $(S_{22})_{ij}/r$ $(j = 1, 2, \cdots, N)$, can be determined by using the following formula

$$\left[\ \frac{(S_{21})_{i1}}{r} \ \cdots\ \frac{(S_{21})_{iN}}{r} \ \vdots\ \frac{(S_{22})_{i1}}{r} \ \cdots\ \frac{(S_{22})_{iN}}{r}\ \right] = [0\ 0 \cdots 0\ -m_i\,]\,[U]^{-1}\,\Phi([A]) \tag{34}$$

where $[U]^{-1}$ is the inverse of the controllability matrix, and

$$\Phi([A]) = [A]^{2N} + \alpha_1[A]^{2N-1} + \alpha_2[A]^{2N-2} + \cdots + \alpha_{2N-1}[A] + \alpha_{2N}[I] \tag{35}$$

in which $\alpha_1, \alpha_2, \cdots, \alpha_{2N-1}, \alpha_{2N}$ are the coefficients of the characteristic polynomial of the desired closed-loop system defined by

$$(\lambda-\bar{\lambda}_1)(\lambda-\bar{\lambda}_2)\cdots(\lambda-\bar{\lambda}_{2N}) = \lambda^{2N}+\alpha_1\lambda^{2N-1} + \alpha_2\lambda^{2N-2} + \cdots + \alpha_{2N} \tag{36}$$

The desired closed-loop poles can also be expressed in terms of natural frequencies and damping ratios. Since the relation between the desired eigenvalues $\bar{\lambda}_{2k-1}$ and $\bar{\lambda}_{2k}$ and the desired natural frequencies $\bar{\omega}_k$ and damping ratios $\bar{\xi}_k$ $(k=1, 2, \cdots, N)$ can be expressed as

$$\left.\begin{aligned} \bar{\lambda}_{2k-1} &= a_k + b_k \\ \bar{\lambda}_{2k} &= a_k - b_k \end{aligned}\right\} \tag{37}$$

where

$$\left.\begin{aligned} a_k &= -\bar{\xi}_k\bar{\omega}_k \\ b_k &= \begin{cases} i\bar{\omega}_k\sqrt{1-\bar{\xi}_k^2} & \text{for } \bar{\xi}_k<1 \\ \bar{\omega}_k\sqrt{\bar{\xi}_k^2-1} & \text{for } \bar{\xi}_k\geq 1 \end{cases} \end{aligned}\right\} \tag{38}$$

then

$$(\lambda-\bar{\lambda}_{2k-1})(\lambda-\bar{\lambda}_{2k}) = \lambda^2 + 2\bar{\xi}_k\bar{\omega}_k + \bar{\omega}_k^2 \quad (0\leq\bar{\xi}_k<\infty) \tag{39}$$

Therefore the nonzero elements in the weighting matrix $[S]$ can also be determined by directly choosing the desired natural frequencies and damping ratios.

After finding the elements $(S_{21})_{ij}$ and $(S_{22})_{ij}$ and $(j=1, 2, \cdots, N)$ and defining the following

distribution factors

$$(\overline{S}_{21})_{ij} = (S_{21})_{ij}/S_0 \text{ and } (\overline{S}_{22})_{ij} = (S_{22})_{ij}/S_0 \tag{40}$$

where $S_0=(S_{22})_{ii}$, the optimum solution can be obtained by trying various ratios of S_0/r.

From Eqs. (37) and (38) it can be seen that if $\overline{\omega}_k$ and $\overline{\xi}_k$ are greater than zero, then the real parts of $\overline{\lambda}_{2k-1}$ and $\overline{\lambda}_{2k}$ will be always less than zero, which implies that the system is stable. Since $\overline{\omega}_k$ and $\overline{\xi}_k$ are always chosen to be positive, it can be concluded that control systems obtained by using the pole placement method are free of the stability problem if the influence of time delays can be neglected.

4. Stability analysis and time-delay correction

Stability analysis determines the stable region for an active control system and examines the influence of parameters of time delays on the stable region (Soong 1990, Chajes 1992). It is of paramount importance because 1) for a system to be stable, the optimal ratio of the weighting matrices, S_0/r, should be located inside the stable region; 2) for some structural parameters, such as natural frequencies and damping ratios which defy perfect accuracy, computation errors are transferred to the deviation of the ratio S_0/r; hence, for the control system to perform robustly, a neighborhood of S_0/r should also be inside the stable region; 3) for any practical control system, time delays exist inevitably; therefore the influence and sensitivity of time delays on a control system as well as their correction must be investigated.

When time delays are considered, the relation between control force $u(t)$ and structural response $\{x(t)\}$ and $\{\dot{x}(t)\}$ can be expressed as

$$\frac{1}{\alpha\omega_l}\dot{u}(t) + u(t) = [G_1]\{x(t-t_x)\} + [G_2]\{\dot{x}(t-t_{\dot{x}})\} \tag{41}$$

where ω_l is the lth natural frequency of the structure; t_x and $t_{\dot{x}}$ are the on-line computational time-delays; and $\alpha = 1/(\omega_l t_b)$, the control force build-up time delay.

By introducing the generalized coordinate vector $\{q(t)\}$ and the modal transformation matrix $[\varphi]$ to the motion equation of an N-story seismic structure with an active tendon installed on a given floor, the following decoupled equation can be obtained

$$[I]\{\ddot{q}(t)\} + [2\xi\omega]\{\dot{q}(t)\} + [\omega^2]\{q(t)\} = [\varphi]^T\{\gamma\}u(t) + [\varphi]^T\{\delta\}\ddot{X}_g(t) \tag{42}$$

where

$$\left.\begin{aligned} \{x(t)\} &= [\varphi]\{q(t)\} \\ [\varphi]^T[M][\varphi] &= [I] \\ [\varphi]^T[C][\varphi] &= [2\xi\omega] \\ [\varphi]^T[K][\varphi] &= [\omega^2] \end{aligned}\right\} \tag{43}$$

By defining

$$\{\dot{q}(t)\} = \{p(t)\} = [I]\{p(t)\} \tag{44}$$

Eqs. (42) and (41) can be written as

$$\{\dot{p}(t)\} = -[\omega^2]\{q(t)\} - [2\xi\omega]\{p(t)\} + [\varphi]^T\{\gamma\}u(t) + [\varphi]^T\{\delta\}\ddot{X}_g(t) \tag{45}$$

$$\dot{u}(t) = \alpha\omega_l \frac{S_1}{r}[\overline{G}_1]\{p(t-t_x)\} + \alpha\omega_l \frac{S_2}{r}[\overline{G}_2]\{p(t-t_{\dot{x}})\} - \alpha\omega_l u(t) \tag{46}$$

where

$$[\bar{G}_k] = -\{\gamma\}^T [M]^{-1}[\bar{S}_{2k}][\varphi] \quad \text{and} \quad [\bar{S}_{2k}] = \frac{1}{S_k}[S_{2k}] \quad (k = 1, 2) \tag{47}$$

Solving the corresponding homogeneous equations of Eqs. (44), (45) and (46) leads to the following characteristic equation

$$\begin{vmatrix} \lambda[I] & -[I] & \{0\} \\ [\omega^2] & \lambda[I]+[2\xi\omega] & \{c\} \\ [a] & [b] & \lambda+\alpha\omega_l \end{vmatrix} = 0 \tag{48}$$

where

$$\left.\begin{aligned} [a] &= -\alpha\omega_l \frac{S_1}{r} e^{-\lambda t_x}[\bar{G}_1] \\ [b] &= -\alpha\omega_l \frac{S_2}{r} e^{-\lambda t_{\dot{x}}}[\bar{G}_2] \\ \{c\} &= -[\varphi]^T\{\gamma\} \end{aligned}\right\} \tag{49}$$

It is known that inside the stable region the real parts of all eigenvalues are negative. Therefore the stability boundaries in the plane of the parameters S_1/r and S_2/r should be determined by points which yield either a zero root (eigenvalue) or a pair of pure imaginary roots of the quasi-polynomial, Eq. (48). The cases of $\lambda=0$ and $\lambda=\pm i\omega$ $(0<\omega<\infty)$ define two bifurcation boundaries between stable foci and unstable foci.

Eq. (48) can be expanded to

$$(\lambda + \alpha\omega_l) - \sum_{j=1}^{N}\left[(a_j+b_j+\lambda)\frac{c_j}{\lambda(\lambda+2\xi_j\omega_j+\omega_j^2)} \right] = 0 \tag{50}$$

Setting $\lambda = 0$ yields

$$\frac{S_1}{r} = \left[\sum_{j=1}^{N} \frac{\bar{g}_{1j} \sum_{k=1}^{N} \varphi_{kj}\gamma_k}{\omega_j^2} \right]^{-1} \tag{51}$$

where $\bar{g}_{1j}$ is the jth element of the matrix $[\bar{G}_1]$ given by Eq. (47). Setting $\lambda=i\omega$ and equating the real and imaginary parts of the resulting equation to zero leads to the following linear equation

$$\begin{bmatrix} A_1 \cos\omega t_x + B_1 \sin\omega t_x & \omega(A_2 \sin\omega t_{\dot{x}} - B_2 \cos\omega t_{\dot{x}}) \\ -A_1 \sin\omega t_x + B_1 \cos\omega t_x & \omega(A_2 \cos\omega t_{\dot{x}} + B_2 \sin\omega t_{\dot{x}}) \end{bmatrix} \begin{Bmatrix} \frac{S_1}{r} \\ \frac{S_1}{r} \end{Bmatrix} = \begin{Bmatrix} -1 \\ -\frac{\omega}{\alpha\omega_l} \end{Bmatrix} \tag{52}$$

where

$$\left.\begin{aligned} A_j &= \sum_{k=1}^{N} \bar{g}_{jk} \frac{(\omega_k^2 - \omega^2)c_k}{(\omega_k^2 - \omega^2)^2 + 4\xi_k^2\omega_k^2\omega^2} \\ B_j &= \sum_{k=1}^{N} \bar{g}_{jk} \frac{-2\xi_k\omega_k\omega c_k}{(\omega_k^2 - \omega^2)^2 + 4\xi_k^2\omega_k^2\omega^2} \end{aligned}\right\} \quad (j = 1, 2) \tag{53}$$

in which $\bar{g}_{jk}$ $(j=1, 2)$ is defined in Eq. (47) and c_k $(k=1, 2, \cdots, N)$ is the kth element of $\{c\}$

given in Eq. (49).

It is noted that the optimal ratio of weighting matrices, S_0/r, is located on the straight line $S_1/r=S_2/r$ of the S_1-S_2 plane. Since the above solution is derived from the homogeneous equation of motion, the stability region obtained may not be exactly the same as that for earthquake excited structures. However, it can be considered a good reference.

If the values of t_x and $t_{\dot{x}}$ can be measured, the influence of time-delays on the relative displacement and velocity of the ith floor, x_i and $\dot{x}_i$ can be corrected by using the following formula:

$$\begin{Bmatrix} x_i' \\ \dot{x}_i' \end{Bmatrix} = \begin{bmatrix} \cos \omega_l t_x & \left[\frac{1}{\omega_l} \sin w_l t_{\dot{x}}\right] \\ -\omega_l \sin \omega_l t_x & \cos \omega_l t_{\dot{x}} \end{bmatrix} \begin{Bmatrix} x_i \\ \dot{x}_i \end{Bmatrix} \tag{54}$$

where x_i' and $\dot{x}_i'$ are the corrected displacement and velocity of the ith floor, respectively, and ω_l is the frequency of the lth mode which is stimulated by the time-delays.

Numerical results indicate that the influence of time delays on the dynamic response mainly exists at adjacent floors of the active tendon. Therefore only those floors' displacements and velocities need to be corrected.

5. Numerical examples

A six-story shear building is used to illustrate the advantages of this generalized active control algorithm. Structural properties are as follows: 1) mass coefficients $m_1=109.78$, $m_2=109.62$, $m_3=109.24$, $m_4=108.86$, $m_5=108.48$, $m_6=107.03$ (tons); 2) stiffness coefficients $k_1=351284$, $k_2=225167$, $k_3=169665$, $k_4=124242$, $k_5=87872$, $k_6=59532$ (kN/m); 3) undamped natural frequencies $\omega_1=9.79$, $\omega_2=24.05$, $\omega_3=37.40$, $\omega_4=49.56$, $\omega_5=63.44$, $\omega_6=83.76$ (rad/sec); 4) 2% structural damping ratio. For dynamic time-history analysis, N-S component of El-Centro earthquake (1940) is employed.

In the following examples, only one active controller is installed on the first floor. In order to show the influence of the $[S]$ matrix configuration on control effectiveness, the ratio S_0/r is selected for the following three types of $[S]$ matrix: 1) diagonal matrix, $S_0=(S)_{ii}$; 2) identical ith row elements of $[S_{21}]$ and $[S_{22}]$, $S_0=S_l$, where $S_l=(S_{2l})_{ij}$ ($l=1, 2$); $j=1, 2, \cdots, 6$ and i is the number of floor where the controller is located; 3) elements $(S_{21})_{ij}$ and $(S_{22})_{ij}$ obtained by using pole placement technique, $S_0=(S_{22})_{ij}$.

Example 1 : In this example, the influence of time-increment Δt on the instantaneous optimal active control (IOAC) and generalized optimal active control (GOAC) algorithms is compared. The weighting matrices $[Q]$ and $[S]$ are formed, with only the first row of $[Q_{21}]$, $[Q_{22}]$, $[S_{21}]$ and $[S_{22}]$ as nonzero elements: $(Q_{21})_{ij}/r=(Q_{22})_{ij}/r=1.2\times10^8$ for IOAC and $(S_{21})_{ij}/r=(S_{22})/r=6.0\times10^5$ for GOAC, ($j=1, 2, \cdots, 6$). Figs. 2(a) and (b) show the influence of Δt on top floor displacement and control force of the structure, respectively. For IOAC algorithm, when two different time-increments, $\Delta t=0.0025$ *sec* and 0.01 *sec* are used, both the displacement and control force associated with these time-increments differ significantly. However, a change in Δt does not influence the response obtained by using GOAC algorithm. Apparently, IOAC is sensitive to time-increment while GOAC is independent of it. In actual engineering practice, both structural response and control force should be free from the selection of Δt.

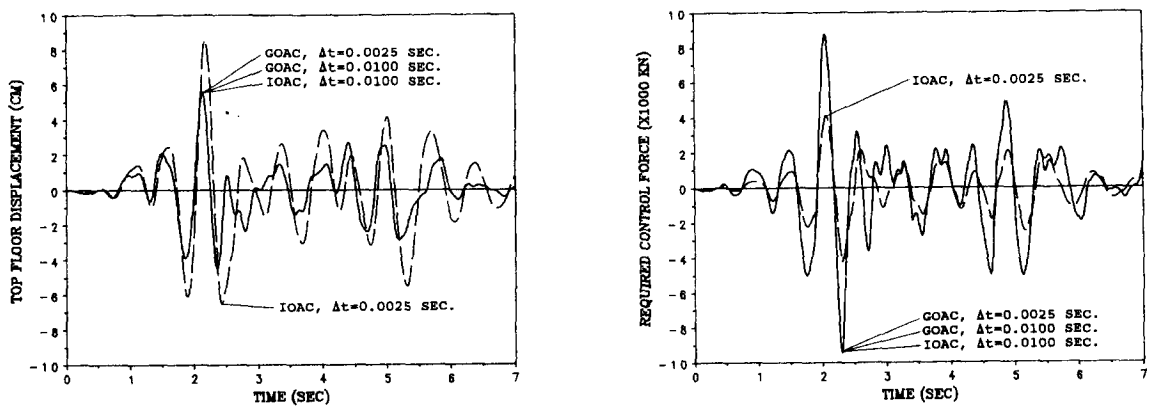

(a) Top Floor Displacement (b) Required Control Force

Fig. 2 Influence of Δt on Displacement and Control Force

Example 2 : This example shows the influence of different selections of $[S]$ matrix on the control effectiveness. In this example, three kinds of $[S]$ matrix are used. For the $[S]$ matrix based on pole placement approach, the desired closed-loop frequencies are selected as $\bar{\omega}_1=15$, $\bar{\omega}_2=25$, $\bar{\omega}_3=35$, $\bar{\omega}_4=50$, $\bar{\omega}_5=65$, $\bar{\omega}_6=80$, *rad/sec*; selecting $\bar{\omega}_1=15$ *rad/sec* is to keep the fundamental frequency of the structure away from the dominant frequency of the applied earthquake, which is about 10.5 *rad/sec*. The desired damping ratios are selected as $\bar{\xi}_1=1.0$, $\bar{\xi}_2=\bar{\xi}_3=\cdots=\bar{\xi}_6=0.5$, for primarily controlling the first mode. Figs. 3(a), (b) and (c) show the influence of S_0/r on maximum displacement, maximum control force and associated performance index for the three kinds of $[S]$ matrix, respectively. Observations may be summarized as follows: 1) for the case of diagonal $[S]$ matrix, maximum displacement can only be reduced a small amount; at the optimal $S_0/r=2\times10^6$, maximum displacement is 92.2% of uncontrolled maximum displacement; raising S_0/r ratio gives a larger control force but does not reduce maximum displacement; 2) for the $[S]$ matrix composed of one row of identical elements, maximum displacement can be significantly reduced; at the optimal $S_0/r=7\times10^5$, maximum displacement is 47.9% of uncontrolled maximum displacement; 3) employing the $[S]$ matrix based on pole placement approach can yield the best control result; at the optimal $S_0/r=3\times10^6$, maximum displacement is reduced to 40.7% of uncontrolled maximum displacement. Table 1 summarizes the influence of different configurations of $[S]$ matrix on optimal results. It is evident that both the maximum displacement and control force obtained by pole placement approach are smaller than those based on the $[S]$ matrix composed of one row of identical elements.

Table 1 Influence of Different Configurations of $[S]$ Matrix on Optimal Results of Example 2.

Types of $[S]$ Matrix	x_m(cm)	u_m(kN)	P.I./(P.I.)$_{max}$
Diagonal	10.77	1550	1.00
Identical Row	5.59	9427	0.25
Pole Placement	4.75	8394	0.21

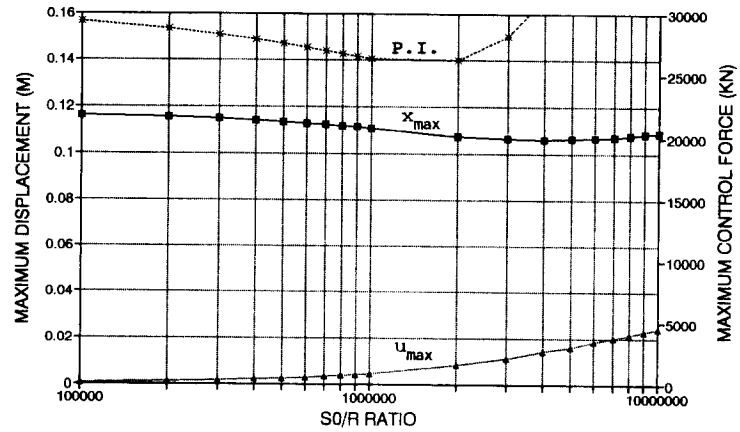

(a) Diagonal [S] Matrix;

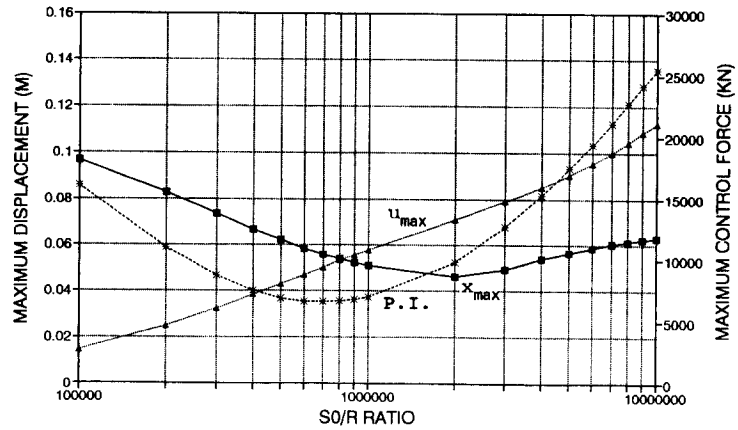

(b) One Row of Identical Elements in [S] Matrix;

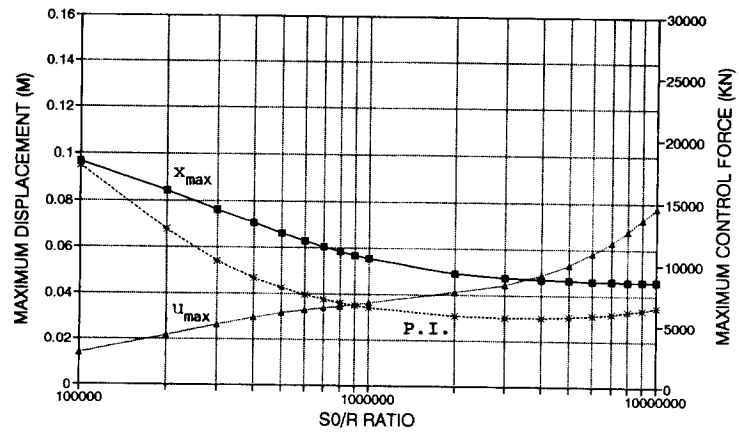

(c) [S] Matrix Using Pole Placement Approach

Fig. 3 Influence of S_0/r Ratio on Maximum Displacement and Control Force

Example 3 : This example shows the influence of the selection of different kinds of [S] matrix and time-delay parameters, t_x, $t_{\dot{x}}$ and α, on the stability region of the control system. Figs. 4(a) and (b) give the stable regions for the [S] matrix composed of one row of identical elements and composed by using pole placement technique, respectively, without taking time-delays into account. Note that for both cases the first quadrant of S_1-S_2 plane is included in the stable regions. Since the parameters S_1 and S_2 are always chosen to be positive, the system should always be stable. It is also worth noting that the stable behavior is a special case and only observed when the control is on the first floor; if the control is on another floor, such as on the fourth floor, a stability region can exist. If time-delays are taken into account, the stability boundary will invade the first quadrant and the system will have stability problems. Figs. 5(a) and (b) give the stability regions with various time-delays. In Fig. 5(a), the stability region is based on the [S] matrix with only one row of identical elements. The control force build-up time-delay α is set to infinity (or $t_b = 0$), and on-line computation time-delays t_x, and $t_{\dot{x}}$ are 0.01, 0.02 and 0.03 *sec*, respectively. Fig. 5(b) shows stability regions based on pole placement approach and various time-delays as $\alpha = \infty$ and $t_x = t_{\dot{x}} = 0.003$, 0.004 and 0.005 *sec*, respectively. From these two figures, it can be seen that stability regions are very sensitive to time-delays. When time-delays increase, the optimal S_0/r ratio of the system is located outside the stable region, and the optimal active control system then becomes unstable. Also note that the more effective the control system is, the more sensitive it will be to time-delays.

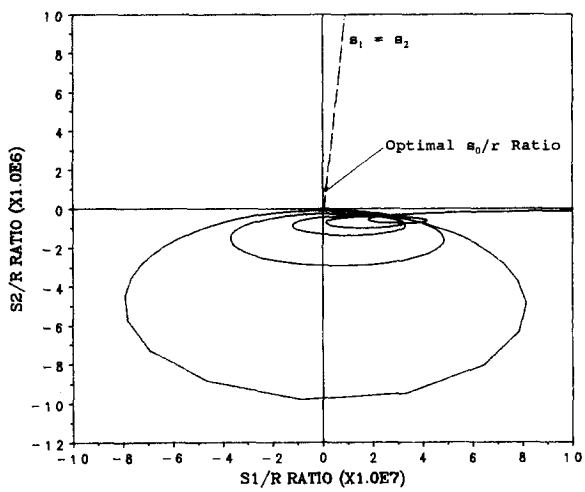

(a) One Row of Identical Elements in [S] Matrix

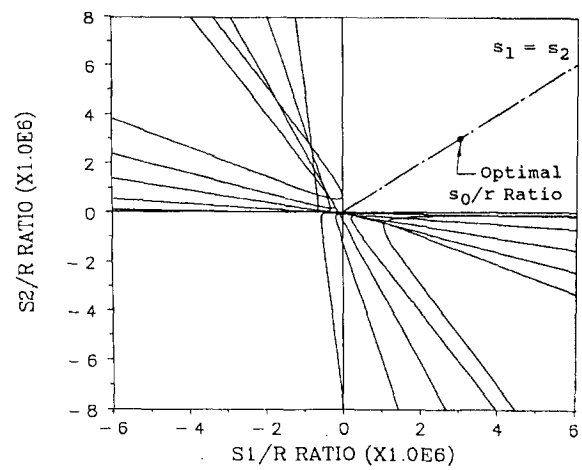

(b) [S] Matrix Using Pole Placement Approach

Fig. 4 Stability Region without Time Delay

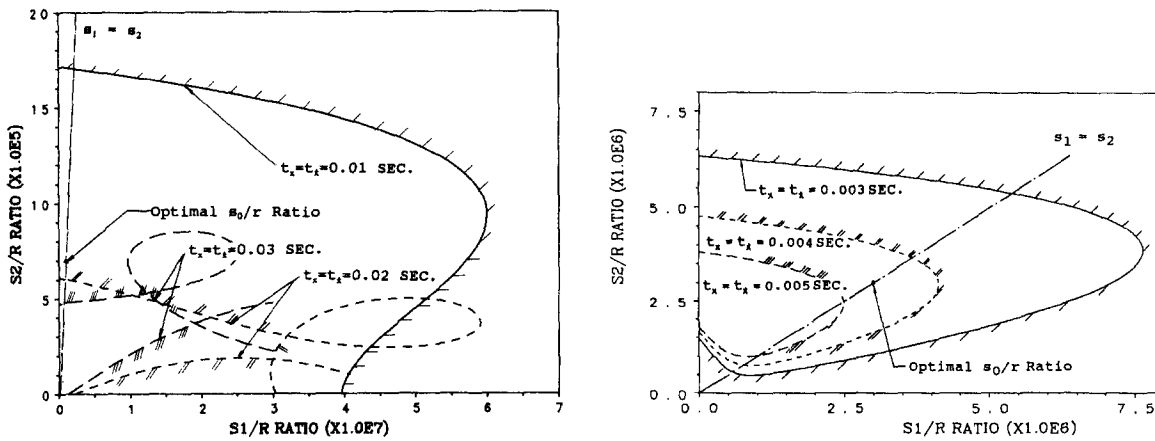

(a) One Row of Identical Elements in [S] Matrix; (b) [S] Matrix Using Pole Placement Approach

Fig. 5 Stability Region with Time Delay

Example 4 : This example demonstrates the influence of time-delays on optimal structural response and required control force. The [S] matrix is based on pole placement approach. Structural response and required control force are evaluated at the optimal $S_0/r=3\times10^6$. Four cases of time-delay are investigated: 1) $t_x=t_{\dot{x}}=0$; 2) $t_x=t_{\dot{x}}=0.003$ *sec*; 3) $t_x=t_{\dot{x}}=0.004$ *sec*; 4) $t_x=t_{\dot{x}}=0.00461$ *sec*. For all four cases, the control force build-up time-delay is ignored with α chosen to be infinity. The results show that the influence of time-delays on the top floor response is sligth, but is significant on the first floor. First floor displacement and required control force are shown in Figs. 6(a) and (b), respectively. The figures reveal that 1) when time-delays are slight ($t_x=t_{\dot{x}}=0.003$, 0.004 sec), their influence on structural response

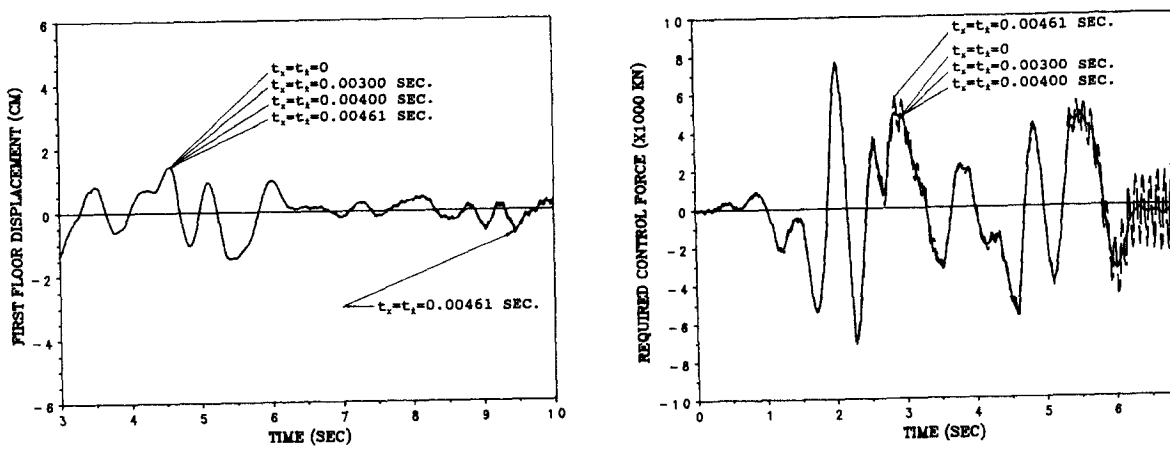

(a) First Floor Displacement; (b) Required Control Force

Fig. 6 Influence of t_x and $t_{\dot{x}}$ on Displacement and Control Force

and required control force is very small; when time-delays t_x and $t_{\dot{x}}$ are increased to 0.00461 *sec*, first floor displacement and control force diverge and the system becomes unstable; 2) for the case of $t_x = t_{\dot{x}} = 0.00461$ *sec*, time-delays affect first floor displacement and control force by fluctuating with very high frequencies and gradually increasing amplitude; 3) control force is more sensitive to time-delay than displacement is.

Example 5 : In this example, the proposed time-delay correction method is employed to show that the effect of time-delays can be significantly reduced through using this approach. Two cases, $t_x = t_{\dot{x}} = 0.00461$ with time-delay correction and without time-delay, are used for comparison. As shown in Figs. 7(a) and (b), amplitudes of dynamic response and control force are reduced almost to the level seen without time-delay, and high-frequency fluctuations are also eliminated.

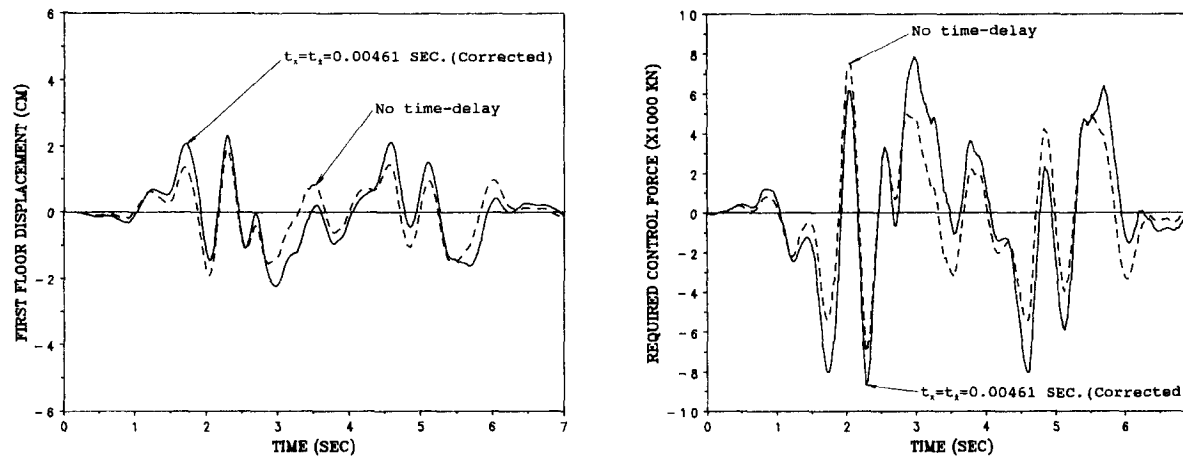

(a) Displacement; (b) Required Control Force

Fig. 7 Effect of Time Delay Correction on Displacement and Control Force

6. Conclusions

This paper presents a generalized optimal active control (GOAC) algorithm, optimal configurations of the weighting matrix based on pole placement technique, the influence of various time delays on the stability region, and the correction of time-delay effects on structural response and control force.

Five numerical examples are provided to show that the proposed optimal active control algorithm is advantageous over others currently in vogue such as instantaneous optimal active control (IOAC) algorithm. In IOAC, feedback control law is dependent on the time increment used in numerical computation while in the GOAC it is not. Compared to the algebraic Riccati algorithm, GOAC offers flexibility in selecting the weighting matrix [S] which can be adjusted at any time during the operation of the control system. Numerical examples also show that the proposed [S] matrix configuration based on pole placement approach is superior to other [S] matrix configurations for it can improve the control effectiveness by adjusting the closed-loop frequencies and damping. The sensitivity of time-delays on stability regions has

also been studied extensively and a correction method is proposed to eliminate the time-delay effect on stability.

Acknowledgements

This research work is partially supported by the National Science Foundation under grants NSF-MSS-9214644 and NSP BCS-9302201 and by the Intelligent Systems Center at UMR. All support for the research is gratefully acknowledged. The findings and conclusions are the opinions of the writers.

References

Abdel-Rohman, M., Quintana, V., and Leipholz, H.H.E. (1980), "Optimal Control of Civil Engineering Structures," *Journal of the Engineering Mechanics Division, ASCE,* **106,** (EM1), 55-73.

Yang, J.N., Akbarpour, A., and Ghaemmaghami, P. (1985), "Optimal Control Algorithms for Earthquake Excited Structures," *Structural Control,* H.H.E. Leipholz (eds.), Martinus, Nijhoff, Proc. 2nd International Symposium on Structural Control, University of Waterloo, Canada, 748-761.

Yang, J.N., Akbarpour, A., and Ghaemmaghami, P. (1987), "Instantaneous Optimal Control Laws for Building Structures Under Earthquake Excitations," *Technical Report,* NCEER-87-0007.

Soong, T.T., et al., (1987), "Experimental Evaluation of Instantaneous Optimal Algorithms for Structural Control," *Technical Report,* NCEER-87-0002.

Soong, T.T. (1990), *Active Structural Control,* Longman, London and Wiley, New York.

Cheng, F.Y. and Pantelides, C.P. (1986), "Optimum Seismic Structural Design with Tendon and Mass Damper Controls and Random Process," *ASCE Structures Congress,* 40-53.

Cheng, F.Y. and Pantelides, C.P. (1986), "Optimization of Structures and Controls under Seismic Loading," *Proc. International Conference on Computational Mechanics,* Tokyo, 135-140.

Cheng, F.Y. and Pantelides, C.P. (1987), "Optimal Active Control of Wind Structures Using Instantaneous Algorithm," *Vibration Control and Active Vibration Suppression,* D.J. Inman and J.C. Simons (eds.), American Society of Mechanical Engineers, 21-28.

Cheng, F.Y. and Pantelides, C.P. (1988), "Algorithm Development for Using Optimal Control in Structural Optimization Subjected to Seismic and Wind Forces," *NSF Report,* U.S. Department of Commerce, National Technical Information Service, NTIS No. PB90-133471/AS.

Cheng, F.Y., Tian, P. and Suthiwong, S. (1991), "Generalized Optimal Active Control Algorithm of Seismic Structures and Related Soil-Structure Formulations," *Computational Mechanics in Structural Engineering, Recent Developments and Future Trends,* F.Y. Cheng and Fu Zizhi (eds.), Elsvier Science Publishers, London and New York 49-62.

Cheng, F.Y. and Tian, P. (1992), "Generalized Optimal Active Control Algorithm for Nonlinear Seismic Structures," *Proc. 10th World conference on Earthquake Engineering,* Madrid, Spain, 3677-3682.

Citron, S.J. (1969), *Elements of Optimal Control,* Holt, Rinehart and Winston, Inc.

Chajes, J.J., Yang, C.Y., and Zhang, L. (1992), "Stability of a 47-story Office Building with Active Controls," *Proc. Structural Stability Research Council,* 237-247.

Ogata, K. (1990), *Modern Control Engineering,* Second Edition, Prentice-Hall, Englewood Cliffs, NJ.